Journal of The Electrochemical Society, **158** (5) A447-A452 (2011)
0013-4651/2011/158(5)/A447/6/$28.00 © The Electrochemical Society

A High Precision Coulometry Study of the SEI Growth in Li/Graphite Cells

A. J. Smith,* J. C. Burns,* Xuemei Zhao, Deijun Xiong, and J. R. Dahn,z**

Department of Physics and Atmospheric Science, Dalhousie University, Halifax, Nova Scotia, Canada B3H3J5

The charge and discharge endpoint capacities as well as the coulombic efficiency of Li/graphite coin cells have been examined using the high precision charger at Dalhousie University. Cells were charged and discharged at different C-rates and temperatures to observe trends in the formation of the solid electrolyte interphase (SEI) on the graphite electrode. The experiments show that time and temperature, not cycle count, are the dominant contributors to the growth of the SEI. The charge consumed by the SEI and hence the SEI thickness, increase approximately with time$^{1/2}$ consistent with a process where the temperature-dependent SEI growth rate is inversely proportional to the SEI thickness. The charge consumed by the SEI is proportional to the electrode surface area and this increased consumption on high surface area electrodes continues during cycling, at least with the 1 M $LiPF_6$ ethylene carbonate:diethyl carbonate electrolyte used.
 [DOI: 10.1149/1.3557892]

Manuscript submitted November 29, 2010; revised manuscript received January 20, 2011. Published March 10, 2011. Publisher error corrected June 16, 2011.

One of the greatest challenges in improving the calendar and cycle life of Li-ion batteries at elevated temperatures is to improve the stability of the passivating film formed on the negative electrode, universally known as the solid electrolyte interphase (SEI). Over the past three decades the formation of these films have been extensively studied by many researchers in an effort to better understand their structure, constituents and how they can be modified.[1–10] Most notably Aurbach et al. have studied the effect of different additives and electrolytes on SEI composition.[7–10] Despite these advancements, fully stable SEI layers have not yet been created and thus the lifetime of Li-ion batteries is not infinite.

As a result of an imperfect SEI on the negative electrode surface and other parasitic reactions, Li-ion batteries experience capacity loss with time, which is aggravated by exposure to elevated temperatures. Many Li ion batteries demonstrate the approximate four-year lifetime required to outlive portable electronics devices that they power. Thus, along with their superior energy densities they have become the ideal battery for these applications. Industrial products such as back-up power supplies, satellites and electric vehicles require significantly longer calendar lives, at least 10 years, and need to be able to operate under challenging environmental conditions. Accelerated testing methods and models have been employed in order to speed up experiments and extrapolate the calendar life of the batteries.[11–21] Many different models explaining the capacity fade of Li ion batteries have been proposed ranging in complexity and detail.[17] However, the majority have related capacity fade to the growth of the negative electrode SEI and the associated rise in overall cell impedance.

Here, the High Precision Charger (HPC) at Dalhousie University[22] was used to study the coulombic efficiency (CE) as well as charge and discharge endpoint capacities of Li/Graphite coin cells cycled at various rates and temperatures. The CE is defined here as the ratio of the charge removed from the negative electrode (graphite) during delithiation divided by the charge transferred to the negative electrode during lithiation. This is a sensitive measure of the amount of Li consumed by SEI growth each cycle. The charge and discharge end point capacities directly track the total irreversible capacity and the total capacity transferred to the graphite electrode, respectively, with cycling. A high precision charger is required to perform these types of measurements – small errors in currents lead to large cumulative errors after many cycles.[22]

The major outcome of this study is that SEI growth continues as cells cycle. The growth rate slows approximately as a function of $t^{-1/2}$, where t is the time since the beginning of cycling. For the parameters investigated, at a particular temperature, the growth rate only depends on t, not on the cycling rate. At a particular temperature, the total amount of lithium incorporated in the SEI (the total irreversible capacity) increases approximately as $t^{1/2}$, again independent of the charge-discharge cycling rate for the parameter range investigated.

Experimental

All cells were tested using the High Precision Charger at Dalhousie University described in Ref. 22. The HPC is a highly accurate battery cycler able to measure the CE of cells cycling slower than C/10 to within ±0.02%. The accumulated error in total irreversible capacity is 0.2% after 10 C/10 cycles and 2% after 100 C/10 cycles.

All Li/graphite cells used in this experiment were made with MCMB (Osaka Gas, heated to ~2650°C), Super-S carbon black (MMM Carbon, Belgium) and a PVDF (Kynar 301F Elf-Atochem) binder. The weight to weight ratios of the active material, carbon black and binder used in the graphite electrodes were 86:7:7, 90:5:5, 92:4:4 or 95:3:2, and are referred to as such throughout the rest of this publication. Before their use all of the electrodes were dried under vacuum at 90°C overnight. The electrolyte used in all of the cells was 1 M $LiPF_6$ in an ethylene carbonate/diethylcarbonate [1:2 v/v, Novolyte Technologies] solution. 2325 coin-type cells with two Celgard 2300 separators and a lithium foil common counter and reference electrode were assembled in an argon-filled glove box with the graphite electrodes described before. All cells were charged and discharged with a constant current between 1.2 and 0.005 V.

To test the reproducibility of the coin cell construction and high precision measurements, five identical cells were made with 92:4:4 electrodes. All of these cells were then cycled at C/20 and at a temperature of 30.0 ± 0.1°C.

In order to observe the different behaviours and trends six Li/graphite cells were made with 86:7:7 electrodes. These cells were then cycled at either C/10 or C/24 and at temperatures of 30.0, 40.0 and 50.0 ± 0.1°C.

Lastly three cells made with either an 86:7:7. 90:5:5 or 95:3:2 electrodes were cycled at C/26 and at a temperature of 30.0 ± 0.1°C. Carbon black has a much larger surface area than graphite so comparing the three electrodes allowed for the impact of total surface area to be studied. Single-point Brunauer–Emmett–Teller (BET) surface area measurements for MCMB, carbon black and the three electrodes (gently removed from their current collectors) were made using a Micromeritics Flowsorb II 2300 surface area analyzer. Samples approximately 500 mg in

* Electrochemical Society Student Member.
** Electrochemical Society Active Member.
z E-mail: jeff.dahn@dal.ca

weight were placed in a glass holder and degassed at 160°C for at least 1 h before the BET measurements.

Results and Discussion

A simple model for SEI growth can be formulated similarly to the growth of oxides on metals. A metal exposed to air reacts to form an oxide which helps passivate the surface and slows further reaction. Similarly, lithiated graphite exposed to electrolyte reacts to form an SEI which helps passivate the surface and slows further reactions. Lawless reviewed numerous models of oxide growth on metals which he showed followed a huge variety of rate laws.[23] The simplest of these is the "parabolic growth law" which assumes that the rate of increase in the thickness of the passivating layer, x, is inversely proportional to the thickness of the layer

$$dx/dt = k/x \quad [1]$$

where k is a proportionally constant. This can be rewritten as

$$xdx = kdt$$

and integrated to give

$$1/2x^2 = kt + C$$

If the thickness is taken to be $x = 0$ at $t = 0$, then the constant, C is zero and one can write

$$x = (2kt)^{1/2} \quad [2]$$

The rate of change of the thickness of the passivating layer is given by combining Eqs. 1 and 2, to give

$$dx/dt = (1/2k)^{1/2}t^{-1/2} \quad [3]$$

In a Li/graphite cell, it is believed that the SEI begins to form as lithium is transferred electrochemically to the graphite electrode. With continued cycling more and more Li is irreversibly consumed as the SEI thickens. The total amount of Li consumed is directly proportional to the SEI thickness, which might be described by Eq. 2, and the amount of lithium consumed by SEI growth is directly proportional to the irreversible capacity each cycle, which might be described by Eq. 3. Therefore, it is important to carefully measure the total accumulated irreversible capacity and the irreversible capacity per cycle and compare them to the predictions of Eqs. 2 and 3. Many researchers studying the failure of Li-ion batteries have identified this capacity loss vs $t^{1/2}$ (or equivalent) relationship and have demonstrated that their models fit experimental data very well.[17,18,20,21]

The High Precision Charger at Dalhousie University can accurately monitor the irreversible capacity growth over many cycles. After 10 C/10 cycles, the total error in accumulated irreversible capacity is only 0.2%. After 100 C/10 cycles it is only 2%. The coulombic efficiency, CE, is related to the irreversible capacity per cycle, q_i, by

$$q_i = (1 - CE)Q \quad [4]$$

where Q is the reversible capacity of the graphite electrode.

Figure 1A shows the cell potential vs specific capacity of one of the 92:4:4 Li/graphite cells used in the reproducibility test. Figure 1B shows the specific capacity vs cycle number for the five cells used in the reproducibility test. There was an excellent agreement between the specific capacities of all of the cells measured at each cycle, with an average standard deviation (SD) of only ±0.9 mAh/g. Figure 1C shows the CE vs cycle number for the same cells. The agreement in the CE measurements was extremely good, and has an average SD of only ±0.0001%. In our opinion, these results are exceptional compared to typical literature results, collected with typical battery cyclers, and they give confidence in the results for the Li/graphite cells.

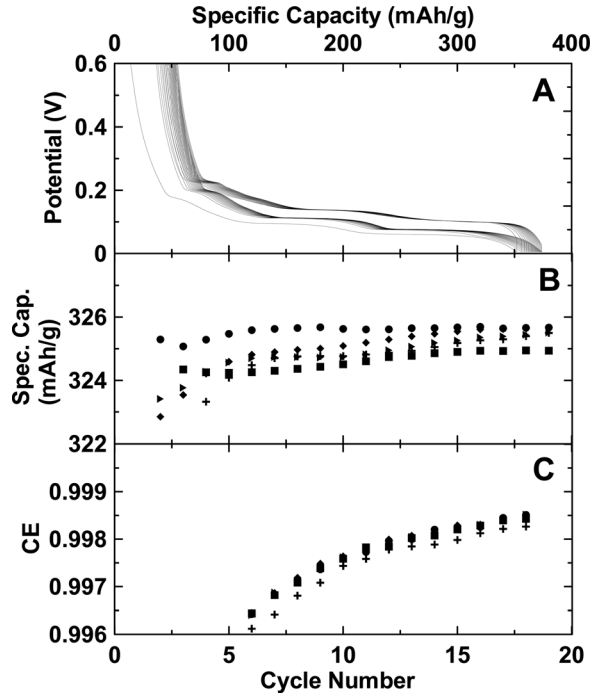

Figure 1. (Panel A) Voltage-specific capacity graph of a Li/graphite coin cell charged and discharged at C/20 and at a temperature of 30°C. The specific capacity vs cycle number (Panel B) and Coulombic Efficiency (CE) vs cycle number (Panel C) of five nominally identical Li/Graphite coin cells charged and discharged at C/10 and 30°C.

Figure 2 shows the charge (removing lithium) and discharge (adding lithium) endpoint capacities, which track the electrode slippage, vs cycle number (top panel) and the cell potential vs capacity (bottom panel) for one of the 86:7:7 cells cycling at C/24 at 40°C.

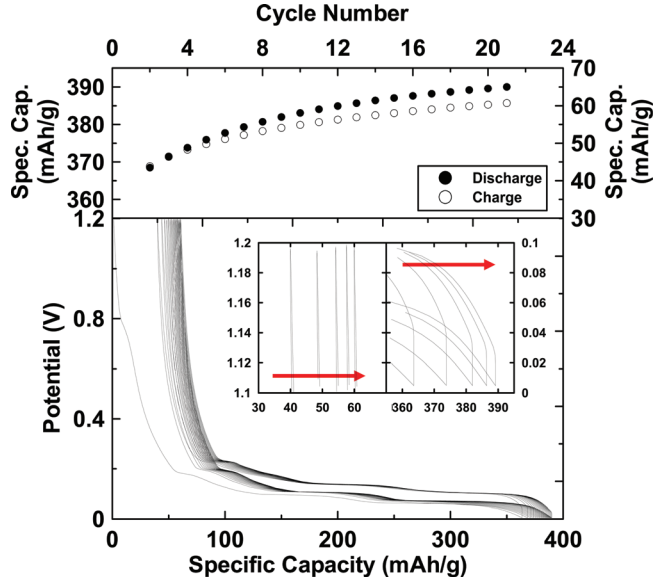

Figure 2. (Color online) (Bottom Panel) Voltage-specific capacity graph of a Li/graphite coin cell charged and discharged at C/24 and at a temperature of 40°C. The inset shows an expanded view of the charge and discharge endpoints, left and right panels respectively, for the second, fourth, sixth, eighth and tenth cycles. (Top Panel) Charge and discharge capacity endpoints vs cycle number.

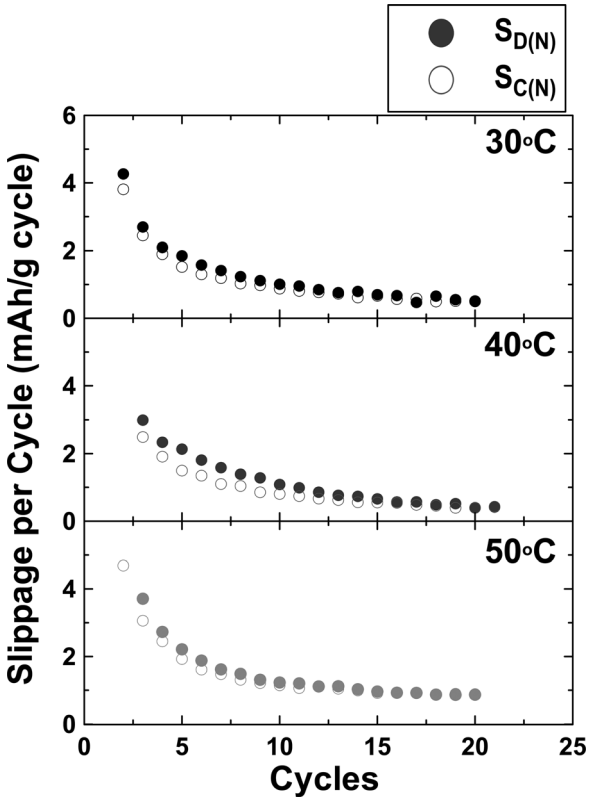

Figure 3. Specific capacity slippage per cycle vs cycle number for the charge and discharge endpoints of Li/Graphite coin cells charged and discharged at C/10 and at different temperatures as indicated.

The smaller insets in the bottom panel show an expanded view of the bottom of discharge (left side) and top of charge (right side) for the second, fourth, sixth, eighth and tenth cycles (arrows expressing the direction of motion). The capacity axis tracks the accumulated capacity of the cells, assuming that the capacity of the cell at the start of the first discharge was 0.00 mAh/g. All endpoints move, or slip, to the right with cycling as is a common feature of all cells we have tested at low rates using the High Precision Charger.[22,24] The total accumulated irreversible capacity vs cycle number is given by the charge and discharge endpoint capacities in the top panel of Fig. 2.

Figure 3 shows the slippage per cycle (how much does the endpoint capacity increase or "slip" per cycle) vs cycle number for the charge ($S_{C(N)}$) and discharge ($S_{D(N)}$) endpoints of the Li/graphite 86:7:7 cells cycling at C/10. The slippage per cycle of all of the cells decreased with increased cycling number but never reached 0.00. This is because the SEI growth rate slows with time but never becomes zero, as predicted by Eq. 3. Figure 3 also shows that the slippages per cycle of the charge and discharge endpoints match closely. This is because the reversible cell capacity, Fig. 1B, is constant for these cells. The charge endpoint slippage per cycle is equal to the growth in irreversible capacity per cycle and is proportional to the amount of lithium consumed in the SEI each cycle. In a case where an excess of Li like this would not be available, such as in a full Li-ion cell, this effect would produce a loss in capacity each cycle.

Figure 4 shows the CE vs cycle number for the Li/graphite 86:7:7 cells cycling at C/10 and C/24 and at temperatures of 30.0, 40.0 and 50.0 ± 0.1°C. The CE of the cells cycling at faster rates was closer to unity than the CE of cells cycling at slower rates. This is because when cells cycle at slower rates, there is more time during each cycle for the SEI to grow and consume charge. Figure 4 also shows that the CE of the cells gets closer to unity with cycling. This is due to the same effect observed in Fig. 3; the SEI thickens and slows the rate of reaction between intercalated lithium and the electrolyte. Thus, as less Li was lost to the SEI each cycle, the cycling efficiency of the cells was improved. Figure 4 also shows that the CE of the cells was affected by temperature. As the temperature was increased, the CE of the cells decreased. This is because parasitic reactions, like SEI growth, are amplified with increased temperatures.

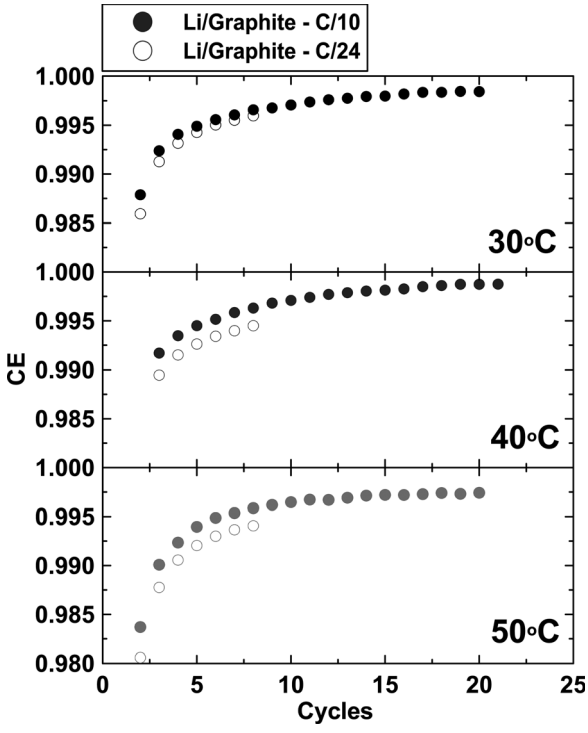

Figure 4. Coulombic Efficiency (CE) vs cycle number for Li/Graphite coin cells charged and discharged at the C-rates and temperatures indicated.

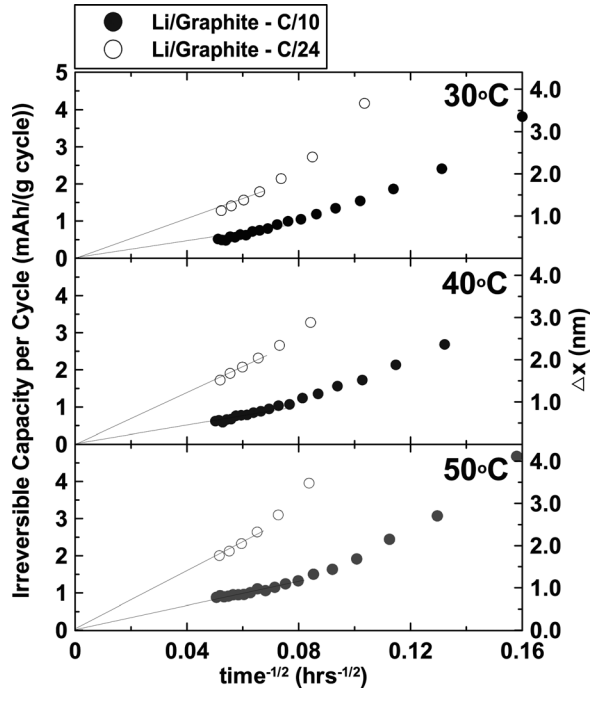

Figure 5. Irreversible specific capacity per cycle plotted vs $t^{-1/2}$ for Li/graphite coin cells cycled at C/10 and C/24 rates at the indicated temperatures. The solid lines are extrapolations to the origin for reader convenience.

Figure 5 shows the irreversible capacity per cycle [$q_i = (1\text{-CE})\ Q$] plotted vs $t^{-1/2}$. The results for all cells become quite linear at large times and appear to extrapolate to the origin at infinite time, as predicted by Eq. 3. The cells which cycle at C/24 have larger irreversible capacities per cycle by about 2.4 times than the cells which cycle at C/10, due to the additional time that SEI thickening reactions can occur in the slowly cycling cells. Figure 6 shows the irreversible capacity per hour, derived from the data in Fig. 5 by dividing by the time of one cycle, plotted vs $t^{-1/2}$. Figure 6 illustrates that the loss of lithium per unit time in cells cycled at the same temperature is independent of the cycling rate. This strongly suggests that the SEI formation reactions occur at the same rate independent of whether the cells are cycled or not.

If it is assumed that the charge consumption in a Li/Graphite cell goes into the thickening of the SEI then, with high quality measurements, one should be able to roughly calculate its growth rate. However these calculations should only be considered approximations, because assumptions about the average molar volume of the Li bi-products forming the SEI, V_m, need to be made. In this case we assumed that the majority of the SEI is formed from C_2H_5LiO, (or Li alkyl carbonates - but we could not find their molar volumes) which has a measured molar volume, V_m, of 5.8×10^{-5} m^3/mole. The increase of the SEI thickness for the Nth cycle, Δx, can then be expressed as follows

$$\Delta x = \frac{3600 C/_{mAh} S_{D(N)} V_m}{A_E F} \quad [5]$$

where A_E is the specific surface area of the electrode, $S_{D(N)}$ is the slippage of the discharge capacity endpoint on the Nth cycle and F is Faraday's constant. The specific surface areas of MCMB and carbon black were measured to be 0.7 and 43.0 m^2/g respectively. As shown in Table I the measured specific surface area of the electrodes did not equal their expected values based on the ratio of their components. Presumably the PVDF was reducing their surface areas. Thus the measured A_E for the 86:7:7, 90:5:5 and 95:3:2 electrodes found to be 2.6, 2.4 and 1.8 m^2/g respectively were the values used in later calculations.

Table I. The expected and measured specific surface areas (SSA) of three graphite electrodes. The weight to weight ratios of the active material (MCMB), carbon black and binder used in the graphite electrodes were 86:7:7, 90:5:5 or 95:3:2. Presumably the PVDF reduces the surface area of the electrodes.

Electrode blending (ratio)	Expected SSA (m^2/g)	Expected SSA divided by SSA of 95:03:02	Measured SSA (m^2/g)	Measured SSA divided by SSA of 95:03:02
86:7:7	3.612	1.85	2.64	1.48
90:5:5	2.78	1.42	2.41	1.35
95:3:2	1.955	1	1.78	1

Figure 5 (right hand axes) shows the variation of Δx vs $t^{-1/2}$. Although there are some major assumptions made about the molar volume of the SEI products, Fig. 5 certainly gives the correct SEI thickness growth rate per cycle to within a factor of 3 or so. After 400 h of testing ($t^{-1/2} = 0.05$), the SEI is still growing at about 0.5 nm per cycle for the cell cycled at C/24 (30°C), or at about 10 pm per h. The growth rate is larger at 50°C as expected.

Figure 7 shows the total accumulated irreversible capacity for the cells described by Figs. 4, 5 and 6 plotted vs $t^{1/2}$ according to the predictions of Eq. 2. The data is quite linear when plotted vs $t^{1/2}$ and the results for cells cycled at either C/10 or C/24 are equivalent, again suggesting that time, not cycle count, is the dominant factor controlling SEI thickening. However, this experiment took only 400 h to complete. It might be suggested that this test was too short to observe the true trends of Li consumption by SEI growth. It is useful to compare our results to the findings of other researchers who have observed similar trends in long term storage experiments.[11–21]

Figure 8 shows data obtained from an impressive paper by Broussely et al. where the aging of prismatic $LiCoO_2$/Graphite cells

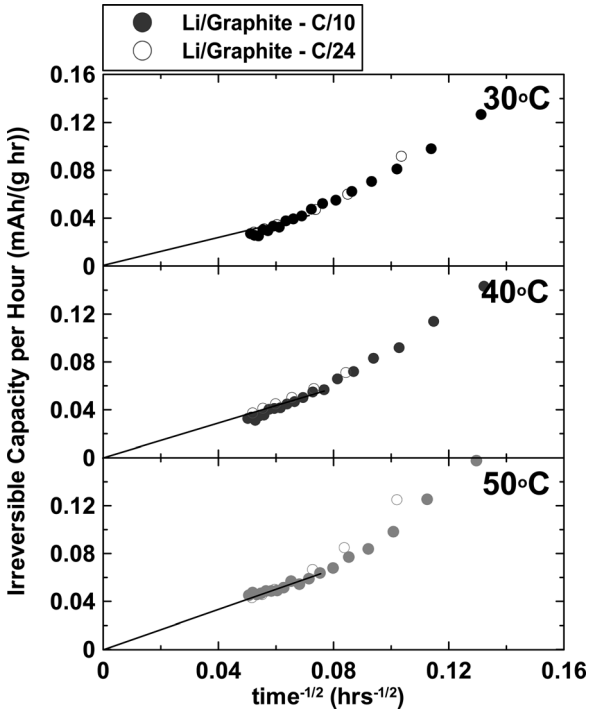

Figure 6. Irreversible specific capacity per hour plotted v $t^{-1/2}$ for Li/graphite cells cycled at C/10 and C/24 rates at the indicated temperatures. The solid lines are extrapolations to the origin for the reader convenience.

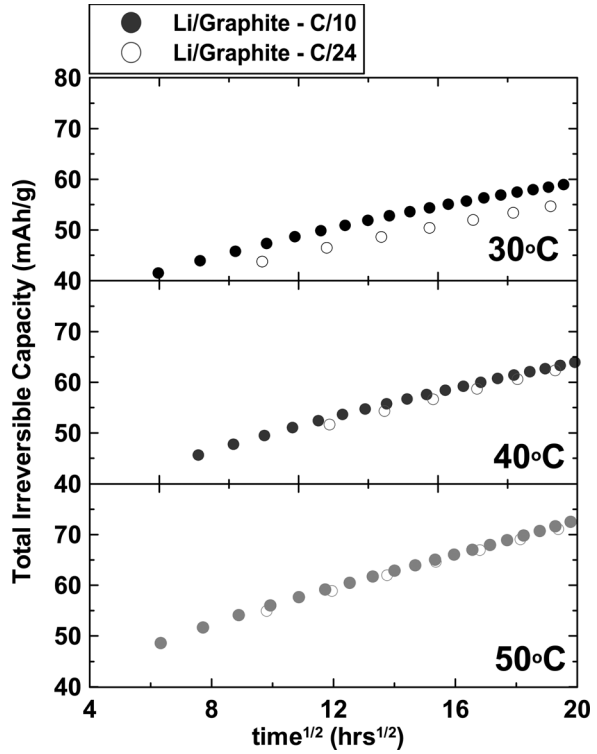

Figure 7. The total irreversible specific capacity plotted vs $t^{1/2}$ for the Li/graphite cells charged and discharged at the C-rates and temperatures indicated.

was observed over a period of 1 year.[14] In their experiment, 5 Ah cells were stored at various temperatures and under an applied voltage, and then their capacities were measured at regular intervals of time. In the original publication (Fig. 7 in Ref. 14) Broussely et al, plotted time vs percent loss of Li due to consumption in the SEI. Broussely et al. did not include the Li lost in the first formation cycle of the cells in their analysis, only that lost upon further storage and cycling. For clarity we have digitized their results and have plotted percent loss of Li vs $t^{1/2}$. When plotted this way, Broussely et al.'s data is roughly linear (Trend lines were added to help guide the eye).

Figure 8 is equivalent to a plot of the accumulated irreversible capacity after the formation cycle (in % of the reversible capacity) vs $t^{1/2}$ for a Li/graphite cell. Our experimental results in Fig. 7 have been re-plotted in this manner on Fig. 8. It is evident that lithium loss is occurring much more rapidly in our coin cells than in the Li-ion cell results from Broussely et al. We believe the major reason for this is caused by the incorporation of significant quantities of carbon black into the 86:7:7 electrodes, which increases their surface area. Figure 8 also shows results for a cell with a 92:4:4 electrode, which loses Li more slowly than the 86:7:7 electrodes, presumably due to the reduced surface area in contact with electrolyte. Although it might be tempting to ascribe that all the differences between our results and those of Broussely et al. to the skill of a battery company (SAFT), we believe much of the difference can be simply explained by a lower carbon black content in the SAFT graphite electrodes. Super S carbon black intercalates Li to about 200 mAh/g and forms an SEI on its surface just like graphite. However, the SAFT cells did incorporate a Vinylene Carbonate (VC) electrolyte additive which is known to affect the SEI on the graphite electrode. The effect of VC additions on the coulombic efficiency of Li/graphite cells is currently under study in our lab. Furthermore, the SAFT cells may have used a different negative electrode binder and this may also affect the reaction rate between the intercalated lithium and the electrolyte. Further experiments on the impact of binder type and amount on the coulombic efficiency of Li/graphite cells is currently under study in our lab.

To further explore the impact of added carbon black to graphite electrodes, Fig. 9 compares precision cycling results for 86:7:7, 90:5:5, and 95:3:2 electrodes at 30°C (C/26 cycling). Figure 9A shows the total accumulated irreversible capacity vs $t^{1/2}$ (top x-axis). Figure 9B shows the irreversible capacity per cycle plotted vs $t^{-1/2}$ (bottom x-axis) and Fig. 9C shows the irreversible capacity per cycle per unit surface area vs $t^{-1/2}$. The 95:3:2 electrode shows less irreversible capacity (Fig. 9A) and a slower growth in irreversible capacity (Fig. 9B). However, when the irreversible capacity growth rate is normalized for the active electrode surface area (Fig. 9C), all the electrodes are equivalent. Therefore, the SEI growth occurs on the graphite and carbon black surfaces at approximately the same rates. The results in Fig. 9 strongly show that negative electrode specific surface area should be minimized in Li-ion cells destined for long-life applications. This, in turn, suggests that much of the "hype" in the literature about the importance of carbon nano tubes, Si nanowires,[25,26] etc. for advanced negative electrodes for Li-ion batteries is simply unfounded.

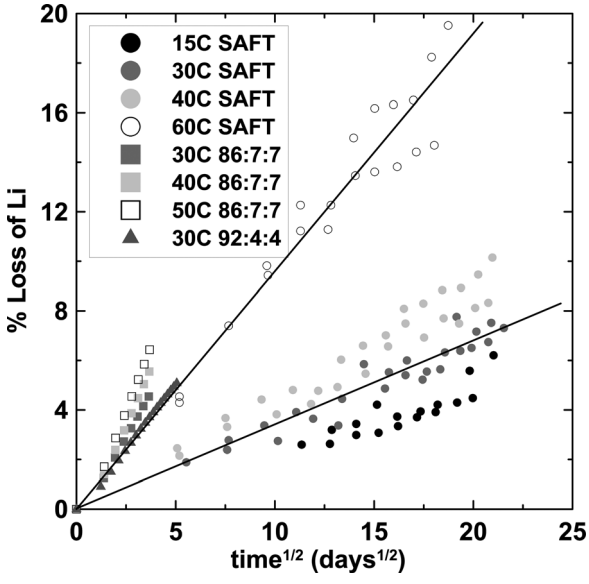

Figure 8. The percentage loss of Li vs $t^{1/2}$ for prismatic $LiCoO_2$/Graphite cells examined in a long term storage test (labeled "SAFT" in the legend). Data were taken from a paper by Broussely et al.[14] The percentage of lithium consumed in the SEI (after the first cycle) compared to the reversible electrode capacity for the Li/graphite cells of this study (labeled "86:7:7 or 92:4:4" in the legend) is also plotted vs $t^{1/2}$.

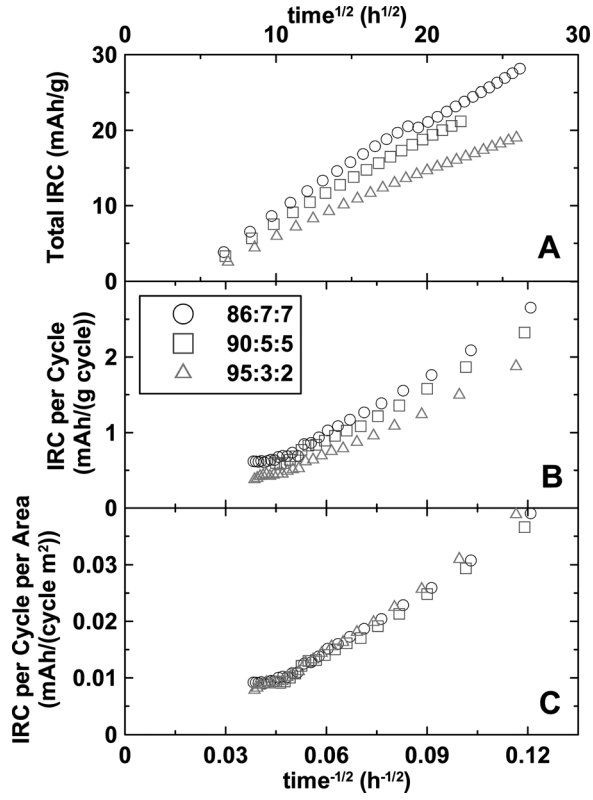

Figure 9. A comparison of precision coulometry results for Li/Graphite cells with 86:7:7, 90:5:5 and 95:3:2 electrodes cycled at C/26 and at a temperature of 30°C. (A) The total accumulated irreversible capacity vs $t^{1/2}$ (top x-axis); (B) The irreversible capacity per cycle plotted vs $t^{-1/2}$ (bottom x-axis); (C) The irreversible capacity per cycle per unit surface area vs $t^{-1/2}$.

Conclusions

The SEI growth rate and consumption of Li on graphite electrodes can be described quite well by a parabolic growth law [Eqs. 1–3]. This, in turn, means that time, not cycle count, dominates the loss of lithium in Li-ion cells cycled at low rates where Li-plating during charge does not occur[24] Of course, this assumes that the potential of the negative electrode is low enough for electrolyte reduction to be occurring. Graphite electrodes have potentials below 0.25 V (vs Li) for over 90% of their state of charge so they satisfy this criterion unless Li-ion cells are carefully discharged to raise the potential of the graphite electrode above the potential for SEI-forming reactions before storage.

High Precision Coulometry allows the loss of lithium to the SEI on graphite electrodes to be effectively studied in a relatively short time frame by contrast to the extended storage and cycling

experiments normally used in the literature. It is our opinion that the effects of electrolyte additives on the SEI can be conveniently studied in simple experiments like those described here, eliminating the need for extensive storage and/or cycling tests. Our results were shown to be similar to literature results collected on cells that were stored and monitored for over 1 year.

Minimizing the negative electrode specific surface area was shown to be a key factor in preventing the continual loss of lithium from Li-ion cells due to continual SEI growth. Many researchers apparently believe that the SEI forms in the first cycle and then its growth stops. We have demonstrated that this is not the case, at least in the temperature range between 30 and 50°C for 1 M $LiPF_6$ EC:DEC electrolyte. Therefore, high surface area negative electrodes will continue to remove active lithium from cells during cycling and storage faster than low surface area electrodes.

It is our opinion that high precision coulometry is a useful tool that should be used widely by Li-ion battery researchers to carefully investigate different electrochemical behaviors in their cells. It is highly unfortunate that commercially available battery cyclers lack the required precision for these experiments at this time. We encourage battery cycler manufacturers to produce equipment with the required precision for these studies.

Acknowledgments

The authors acknowledge NSERC and 3M Canada for funding this work under the auspices of the Industrial Research Chairs program. The authors thank Dr. Jamie Gardner and Dr. Bob Visser for their personal interest in this project.

Dalhousie University assisted in meeting the publication costs of this article.

References

1. E. Peled, *J. Electrochem. Soc.*, **126**, 2047 (1979).
2. E. Peled, D. Golodnitsky, and G. Ardel, *J. Electrochem. Soc.*, **144**, L208 (1997).
3. K. Xu, U. Lee, S. S. Zhang, and T. R. Jow, *J. Electrochem. Soc.*, **151**, A2106 (2004).
4. R. Fong, U. Sacken, and J. R. Dahn, *J. Electrochem. Soc.*, **137**, 2009 (1990).
5. Z. Ogumi and M. Inaba, *Bull. Chem. Soc. Jpn.*, **71**, 521 (1998).
6. F. Kong, J. Kim, X. Song, M. Inaba, K. Kinoshita, and F. McLarnon, *Electrochem. Solid-State Lett.*, **1**, 39 (1998).
7. D. Aurbach, Y. Gofer, and J. Langzam, *J. Electrochem. Soc.*, **136**, 3198 (1989).
8. D. Aurbach, M. L. Daroux, P. W. Faguy, and E. Yeager, *J. Electrochem. Soc.*, **134**, 1611 (1987).
9. D. Aurbach, Y. Ein-Eli, O. C. Youngman, Y. Carmeli, M. Babai, and H. Yamin, *J. Electrochem. Soc.*, **141**, 603 (1994).
10. D. Aurbach, E. Zinigrad, Y. Cohen, and H. Teller, *Solid State Ionics*, **148**, 405 (2002).
11. K. Araki and N. Sato, *J. Power Sources.*, **124**, 124 (2003).
12. R. B. Wright, C. G. Motloch, J. R. Belt, J. P. Christophersen, C. D. Ho, R. A. Richardson, I. Bloom, S. A. Jones, V. S. Battaglia, G. L. Henriksen, et al., *J. Power Sources.*, **110**, 445 (2002).
13. M.-Q Li, M.-Z Qu, X.-Y. He, and Z.-L. Yu, *Electrochim. Acta*, **54**, 4506 (2009).
14. M. Broussely, S. Herreyre, Ph. Biensan, P. Kasztejna, K. Nechev, and R. J. Staniewicz, *J. Power Sources.*, **97**, 13 (2001).
15. I. Bloom, B. W. Cole, J. J. Sohn, S. A. Jones, E. G. Polzin, V. S. Battaglia, G. L. Henriksen, C. Motloch, R. Richardson, T. Unkelhaeuser, *et al.*, *J. Power Sources.*, **101**, 238 (2001).
16. R. B. Wright, J. P. Christophersen, C. G. Motloch, J. R. Belt, C. D. Ho, V. S. Battaglia, J. A. Barnes, T. Q. Duong, and R. A. Sutula, *J. Power Sources.*, **119**, 865 (2003).
17. R. Spontiz, *J. Power Sources.*, **113**, 72 (2003).
18. G. E. Blomgren, *J. Power Sources.*, **81–82**, 112 (1999).
19. S. Watanabe, M. Kinoshita, and K. Nakura, Abstract 655, The 15th International Meeting on Lithium Batteries - IMLB 2010 Montreal, Canada, June 27–July 2, 2010.
20. P. Ramadass, B. Haran, R. White, and B. N. Popov, *J. Power Sources.*, **123**, 230 (2003).
21. T. Yoshida, M. Takahashi, S. Morikawa, C. Ihara, H. Katsukawa, T. Shiratsuchi, and J. Yamakic, *J. Electrochem. Soc.*, **153**, A576 (2006).
22. A. J. Smith, J. C. Burns, S. Trussler, and J. R. Dahn, *J. Electrochem. Soc.*, **157**, A196 (2010).
23. K. R. Lawless, *Rep. Prog. Phys.*, **37**, 231 (1974).
24. A. J. Smith, J. C. Burns, and J. R. Dahn, *Electrochem. Solid-State Lett.*, **13**, A177 (2010).
25. M.-H. Park, M. G. Kim, J. Joo, K. Kim, J. Kim, S. Ahn, Y. Cui, and J. Cho, *Nano Lett.*, **9**, 3844 (2009).
26. X. Li, F. Kang, X. Bai, and W. Shen, *Electrochem. Commun.*, **9**, 663 (2007).